Flow of Spatiotemporal Turbulentlike Random Fields

Jason Reneuve[1,*] and Laurent Chevillard[2]
[1]Laboratoire des Ecoulements Géophysiques et Industriels, Université Grenoble Alpes, CNRS, Grenoble-INP, F-38000 Grenoble, France
[2]Université Lyon, Ens de Lyon, Université Claude Bernard, CNRS, Laboratoire de Physique, 46 allée d'Italie, F-69342 Lyon, France

(Received 7 April 2020; revised 12 May 2020; accepted 3 June 2020; published 1 July 2020)

We study the Lagrangian trajectories of statistically isotropic, homogeneous, and stationary divergence-free spatiotemporal random vector fields. We design this advecting Eulerian velocity field such that it gets asymptotically rough and multifractal, both in space and time, as it is demanded by the phenomenology of turbulence at infinite Reynolds numbers. We then solve numerically the flow equations for a differentiable version of this field. We observe that trajectories get also rough, characterized by nearly the same Hurst exponent as the one of our prescribed advecting field. Moreover, even when considering the simplest situation of the advection by a fractional Gaussian field, we evidence in the Lagrangian framework additional intermittent corrections. The present approach involves properly defined random fields, and asks for a rigorous treatment that would explain our numerical findings and deepen our understanding of this long lasting problem.

DOI: 10.1103/PhysRevLett.125.014502

A powerful and physically insightful way to characterize many dynamical systems, such as those encountered in fluid mechanics, consists in studying the path lines $\boldsymbol{X}(t)$ of a given advecting field $\boldsymbol{u}(\boldsymbol{x},t)$, at the position $\boldsymbol{x}\in\mathbb{R}^d$ and time $t>0$, defined by

$$\frac{d\boldsymbol{X}(t)}{dt}=\boldsymbol{u}(\boldsymbol{X}(t),t). \tag{1}$$

In the context of fluid turbulence, where the velocity field $\boldsymbol{u}$ is governed by the Navier-Stokes equations, such Lagrangian trajectories of fluid particles have been extensively studied in laboratory and numerical flows [1–13]. In this situation, the three-dimensional Eulerian advecting flow $\boldsymbol{u}$ is incompressible (i.e., divergence free) and exhibits a complex multiscale structure in both space [14] and time [15]. In particular, in the fully developed turbulent regime concerning the asymptotic limit of infinite Reynolds numbers, $\boldsymbol{u}$ gets rough (i.e., nondifferentiable) in both space and time, and characterized in a statistically averaged sense by a Hurst exponent of order $H_{\mathrm{Eul}}\approx 1/3$. In the phenomenology of turbulence mostly developed by Kolmogorov [16], this can be broadly understood on dimensional grounds if it is assumed that the average dissipation by unit of mass remains finite at infinite Reynolds numbers [14]. Similarly, the Lagrangian velocity $\boldsymbol{v}(t)\equiv\boldsymbol{u}(\boldsymbol{X}(t),t)$, i.e., the velocity of a tracer advected by the flow $\boldsymbol{u}$, develops small scales such that it gets rough and characterized by a Hurst exponent of order $H_{\mathrm{Lag}}\approx 1/2$. Again, under the same assumption, this exponent can be obtained from dimensional arguments, and says that Lagrangian velocity has the same regularity as the one of a Brownian motion [15].

Whereas it remains elusive to derive these behaviors from first principles, we propose in this Letter to study the statistical properties of Lagrangian trajectories extracted from a prescribed advecting velocity field that reproduces some of the main aforementioned features of turbulence. A similar approach has been already explored for various random vector fields [17–21], although, as we will see, our advecting flow is more general, in particular concerning possible intermittent corrections.

In order to draw the simplest and numerically tractable picture of these phenomena, we need to come up with a proposition for the prescribed advecting velocity field $\boldsymbol{u}(\boldsymbol{x},t)$. Recall that we want it to be divergence free at any time to ensure statistical stationarity of induced Lagrangian velocities [22]. For this reason, we will consider henceforth a two-component vector field $\boldsymbol{u}=(u_1,u_2)$ living in a two-dimensional space $\boldsymbol{x}=(x_1,x_2)\in\mathbb{R}^2$ and for $t\in\mathbb{R}$, such that $\boldsymbol{\nabla}\cdot\boldsymbol{u}=0$ at any time. In an asymptotic regime, mimicking the behavior of turbulence at infinite Reynolds numbers, this vector field is eventually rough, governed in a statistically averaged sense by a Hurst exponent $H\in]0,1[$ (taken to be $1/3$ as far as turbulence is concerned). A first step in this direction would be to consider fractional Gaussian fields, defined as linear operations on a space-time white noise (similarly to the approach developed in [23–27]), regularized over a small parameter $\epsilon>0$ ensuring differentiability in both space and time (compatible in particular with the divergence-free condition). Going beyond this Gaussian framework, we

would like also to consider some intermittent (i.e., multifractal) corrections [14], and to explore their implication on the statistical behavior of Lagrangian trajectories. To make our notations lighter, without loss of generality, we consider in the sequel nondimensional space and time coordinates.

Along these lines, the simplest random vector field that we have in mind, which is statistically stationary, isotropic, and homogeneous, and which reproduces these statistical behaviors, is given by

$$\boldsymbol{u}(\boldsymbol{x},t)=\int_{\boldsymbol{y}\in\mathbb{R}^2,s\in\mathbb{R}}\boldsymbol{\mathcal{G}}_{\epsilon,H_{\mathrm{Eul}}}(\boldsymbol{x}-\boldsymbol{y},t-s)M_{\epsilon,\gamma_{\mathrm{Eul}}}(d^2y,ds), \quad (2)$$

where the vector kernel $\boldsymbol{\mathcal{G}}_{\epsilon,H_{\mathrm{Eul}}}$ acting linearly on the random measure $M_{\epsilon,\gamma_{\mathrm{Eul}}}$ (specified later) reads

$$\boldsymbol{\mathcal{G}}_{\epsilon,H_{\mathrm{Eul}}}(\boldsymbol{x},t)=\varphi(\boldsymbol{x},t)\frac{\boldsymbol{x}^{\perp}}{||\boldsymbol{x},0||_{\epsilon}}||\boldsymbol{x},t||_{\epsilon}^{H_{\mathrm{Eul}}-3/2}, \quad (3)$$

with $||\boldsymbol{x},t||_{\epsilon}^2=|\boldsymbol{x}|^2+t^2+\epsilon^2$ a regularized spatiotemporal norm over ϵ and $\boldsymbol{x}^{\perp}=(-x_2,x_1)$. Note that we implicitly assume that in our nondimensional reference frame, the small scale ϵ plays the role of both the spatial and temporal dissipative scales. This is consistent with the similar dependence of the so-called Kolmogorov length scale η_K and the sweeping timescale [15] on the Reynolds number. The scalar cutoff function φ ensures that this field has a finite variance. It goes smoothly to zero as $|\boldsymbol{x}|$ gets of the order of the integral length scale L and/or t of the order of the integral timescale T. Once expressed in our nondimensional coordinate system, we take $L=T$ and assume $\varphi(\boldsymbol{x},t)=\exp\{-[(|\boldsymbol{x}|^2+t^2)/2L^2]\}$. The very form of the kernel $\boldsymbol{\mathcal{G}}$ [Eq. (3)] is inspired by the two-dimensional Biot-Savart law [28], and ensures that the velocity field [Eq. (2)] is divergence free for any finite $\epsilon>0$ and at any time. Additional technical details are provided in [29].

The random spatiotemporal measure $M_{\epsilon,\gamma_{\mathrm{Eul}}}$ reads

$$M_{\epsilon,\gamma_{\mathrm{Eul}}}(d^2y,ds)=e^{\gamma_{\mathrm{Eul}}Y_{\epsilon}(\boldsymbol{y},s)-\gamma_{\mathrm{Eul}}^2\langle Y_{\epsilon}^2\rangle}W(d^2y,ds), \quad (4)$$

where W is a spatiotemporal Gaussian white noise (thus $2+1$ dimensional) and Y_{ϵ} a zero-average scalar Gaussian random field, logarithmically correlated in both space and time as $\epsilon\to 0$, taken as independent of W. As we will see, the parameter γ_{Eul} governs entirely the intermittent corrections, and $M_{\epsilon,\gamma_{\mathrm{Eul}}}$ can be viewed as a continuous, statistically homogeneous and stationary version of the discrete cascade models [32–34]. Being Gaussian, the scalar field Y_{ϵ} can be obtained as a linear operation on an independent white noise $\tilde{W}$, that is $Y_{\epsilon}(\boldsymbol{x},t)=(1/\sqrt{4\pi})\int_{\boldsymbol{y},s}\mathcal{H}_{\epsilon}(\boldsymbol{x}-\boldsymbol{y},t-s)\tilde{W}(d^2y,ds)$ with $\mathcal{H}_{\epsilon}(\boldsymbol{x},t)=||\boldsymbol{x},t||_{\epsilon}^{-3/2}1_{|\boldsymbol{x}|^2+t^2\le L^2}$ and 1_S the indicator function of the set S.

Using similar technics as in Refs. [23–27], in particular calling for stochastic calculus methods developed for multiplicative chaos theory [35], it can be shown that the velocity field $\boldsymbol{u}$ [Eq. (2)] is rough in the limit of vanishing regularizing scale $\epsilon\to 0$, such that for instance the moments of the longitudinal velocity increments $\delta_{\ell}u_1(\boldsymbol{x},t)=u_1(x_1+\ell,x_2,t)-u_1(x_1,x_2,t)$ (i.e., the structure functions) behave for $q\ge 1$, $H_{\mathrm{Eul}}\in]0,1[$ and $\gamma^2\le H_{\mathrm{Eul}}/(q-1)$, as

$$\lim_{\epsilon\to 0}\langle(\delta_{\ell}u_1)^{2q}\rangle\underset{\ell\to 0^+}{\sim}C_{2q,H_{\mathrm{Eul}},\gamma_{\mathrm{Eul}}}\ell^{2qH_{\mathrm{Eul}}-2q(q-1)\gamma_{\mathrm{Eul}}^2}, \quad (5)$$

where the multiplicative factor $C_{2q,H,\gamma_{\mathrm{Eul}}}$ is finite and positive. The scaling behavior entering in Eq. (5) indicates that $\boldsymbol{u}$ [Eq. (2)] is intermittent and exhibits a quadratic (i.e., log-normal) spectrum. The respective transverse (i.e., the scale ℓ is taken along the second direction) and temporal (i.e., we look at the increment over a time τ at a fixed position) structure functions behave similarly as in Eq. (5), with the same spectrum of exponents but with different multiplicative constants. More general spectra than the quadratic one could be considered [35–38], although calculations leading to the exact asymptotic result Eq. (5) get more intricate, and the quadratic spectrum reproduces a convincing phenomenology of intermittency at low statistical orders.

Numerical simulations of $\boldsymbol{u}$ [Eq. (2)] are performed in a $(2+1)$-dimensional periodic box of unit length and duration using $N=2^{11}$ collocations points in each direction, such that $dx=dt=1/N$. Convolutions of the deterministic functions $\boldsymbol{\mathcal{G}}_{\epsilon,H}$ [Eq. (3)] and $\mathcal{H}_{\epsilon}$ [i.e., the kernel of Y_{ϵ} entering in Eq. (4)] with two independent instances W and $\tilde{W}$ of variance dx^2dt of the white noise are computed in an efficient way in the Fourier domain. We use for the large scales $L=T=1/4$. The singular kernels $\boldsymbol{\mathcal{G}}_{\epsilon,H}$ and $\mathcal{H}_{\epsilon}$ are regularized over the small scale $\epsilon=4dx$ such that, up to numerical errors, the obtained field $\boldsymbol{u}$ is differentiable in space and time, and divergence free in particular. Finally, the trajectories $\boldsymbol{X}(t)$ of 2^{14} particles, initially uniformly distributed in the unit square, are computed according to Eq. (1) using a second-order Runge-Kutta time marching scheme and linear interpolation of the velocities, as detailed in Ref. [39]. Their respective Lagrangian velocity $\boldsymbol{v}(t)=d\boldsymbol{X}(t)/dt$ and acceleration $\boldsymbol{a}(t)=d^2\boldsymbol{X}(t)/dt^2$ are obtained using finite-difference time derivatives.

Let us first focus on the statistical analysis of the trajectories in an advecting Gaussian velocity field $\boldsymbol{u}(\boldsymbol{x},t)$ [Eq. (2)]. To do so, we consider the nonintermittent case $\gamma_{\mathrm{Eul}}=0$, and the particular value $H_{\mathrm{Eul}}=1/3$ to mimic the regularity of turbulence. We display in Fig. 1(a) the trajectories of particles initially uniformly distributed in the unit square. We indeed observe strong chaotic mixing, and notice that during the unit duration of the simulation, particles have traveled a distance of order unity, as expected. We show in Fig. 1(c) a typical time series of

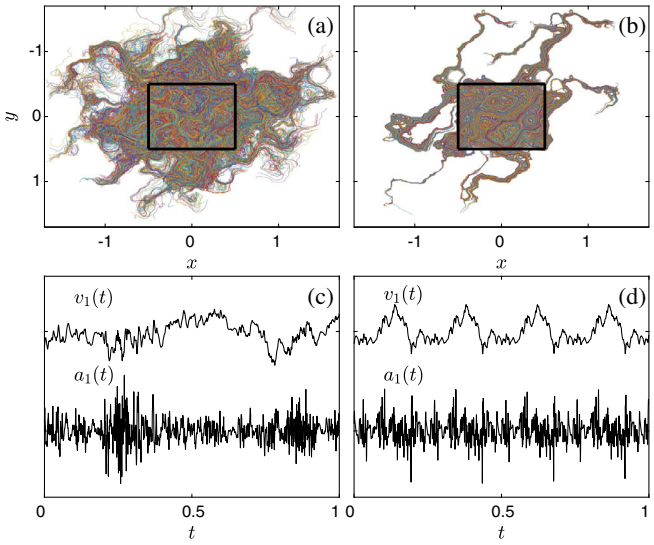

FIG. 1. Path lines $\boldsymbol{X}(t)$ [Eq. (1)] of a Gaussian velocity field $\boldsymbol{u}(\boldsymbol{x},t)$ [Eq. (2)], using $H_{\mathrm{Eul}}=1/3$ and $\gamma_{\mathrm{Eul}}=0$. Other parameters of the simulation are given in the text. (a) Each of the trajectories are represented with various colors, starting initially from positions uniformly distributed in the unit square centered on the origin (and represented with thick black lines). (c) Typical time series of velocity v_1 and acceleration a_1 of a particle. Series are arbitrarily shifted horizontally and renormalized such that they are of same variance. (b) and (d) Similar plot as in (a) and (c), but for a frozen-in-time velocity field $\boldsymbol{u}(\boldsymbol{x},0)$.

velocity $v_1(t)$ and acceleration $a_1(t)$ over the duration of the simulation. We can see that the series are indeed statistically stationary. Also, v_1 is correlated over the large integral timescale T, whereas a_1 gets correlated over the small timescale ϵ, which is consistent with the phenomenology of turbulence. A trained eye would see that a clearly deviates from Gaussianity.

At this stage, it is tempting to explore the statistics of the trajectories obtained while advecting the tracers by a frozen-in-time velocity field, say $\boldsymbol{u}(\boldsymbol{x},0)$. We represent in Fig. 1(b) the respective trajectories. Mixing is there much less efficient than for the time-evolving velocity field [Fig. 1(a)]. In particular, many of them have closed orbits. Typical time series of v_1 and a_1 on a closed orbit are shown in Fig. 1(d), displaying an expected periodicity.

Let us now estimate the regularity of $\boldsymbol{v}(t)$ obtained from a Gaussian velocity field $\boldsymbol{u}(\boldsymbol{x},t)$ [Eq. (2) with $\gamma_{\mathrm{Eul}}=0$], and quantify its dependence on H_{Eul}. To do so, we perform simulations using ten values for H_{Eul} between 0.1 and 0.9. Subsequent statistics are obtained using 2^{14} trajectories from ten independent realizations of the random Eulerian field. To quantify the regularity of $\boldsymbol{v}$, we estimate the moments of the velocity time increments $\delta_\tau^1 v_1(t)=v_1(t+\tau)-v_1(t)$, and define the respective Lagrangian Hurst exponent H_{Lag} and intermittency coefficient γ_{Lag} as

$$\langle(\delta_\tau^1 v_1)^{2q}\rangle \underset{\epsilon\ll\tau\ll T}{\propto} \tau^{2qH_{\mathrm{Lag}}-2q(q-1)\gamma_{\mathrm{Lag}}^2}, \tag{6}$$

such that H_{Lag} can be estimated while fitting in the inertial range (i.e., for $\epsilon\ll\tau\ll T$) the power-law exponent of $\langle(\delta_\tau^1 v_1)^2\rangle\propto\tau^{2H_{\mathrm{Lag}}}$. More generally, let us note that whereas the behavior of Eulerian structure functions [Eq. (5)] is exact in the asymptotic limit of vanishing ϵ and scale ℓ, the proposed behavior of their Lagrangian counterparts [Eq. (6)] is a model whose parameters $(H_{\mathrm{Lag}},\gamma_{\mathrm{Lag}}^2)$ will be eventually estimated following a fitting procedure.

We display in Fig. 2(a) the dependence on the scale τ of the second-order structure function in a logarithmic representation, for the ten values of the Eulerian Hurst exponent H_{Eul}. We indeed observe a power-law behavior between the dissipative range $\tau\ll\epsilon$, where $\langle(\delta_\tau^1 v_1)^2\rangle\propto\tau^2$ and the large scales $\tau\gg T$ for which we get a saturation toward $2\langle v_1^2\rangle$. We proceed with the fit of the power-law exponent (represented by solid black lines) and gather our results in Fig. 2(c) (using $\circ$). We can see that the estimated regularity of Lagrangian trajectories H_{Lag} is very close to the imposed Eulerian regularity H_{Eul}, that is $H_{\mathrm{Lag}}\approx H_{\mathrm{Eul}}$, as it was observed in the synthetic three-dimensional, slowly evolving in time, flow of Ref. [21] and in the frozen Navier-Stokes field of Ref. [40]. We superimpose with a dashed line such a prediction, showing that is does reproduce some of our estimations when H_{Eul} is smaller than $1/2$. Since the level of regularity is high, it is tempting

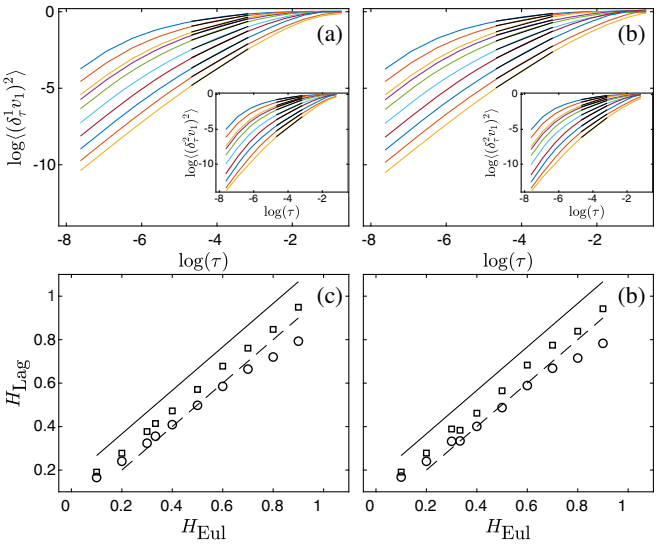

FIG. 2. (a) Logarithmic representation of the second-order Lagrangian structure function $\langle(\delta_\tau^1 v_1)^2\rangle/(2\langle v_1^2\rangle)$ [Eq. (6)] obtained from a Gaussian velocity field $\boldsymbol{u}(\boldsymbol{x},t)$ [Eq. (2)] using $\gamma_{\mathrm{Eul}}=0$ and $H_{\mathrm{Eul}}=0.1,0.2,0.3,1/3,0.4,0.5,0.6,0.7,0.8$, and 0.9 (from top to bottom). Results of our fitting procedure are displayed with black lines. Inset: Similar plot as in (a), but for the second-order velocity increment moment $\langle(\delta_\tau^2 v_1)^2\rangle/(6\langle v_1^2\rangle)$. (b) Same plot as in (a), but for the frozen-in-time advecting field $\boldsymbol{u}(\boldsymbol{x},0)$. (c) Power-law exponents observed in (a), i.e., $2H_{\mathrm{Lag}}$, estimated using $\langle(\delta_\tau^1 v_1)^2\rangle$ ($\circ$) and $\langle(\delta_\tau^2 v_1)^2\rangle$ ($\square$). We superimpose the two discussed behaviors $H_{\mathrm{Lag}}=H_{\mathrm{Eul}}$ (dashed line) and $H_{\mathrm{Lag}}=H_{\mathrm{Eul}}+\frac{1}{6}$ (solid line). (d) Same plot as in (c), but for $\boldsymbol{u}(\boldsymbol{x},0)$.

to check whether similar results are obtained with the second-order increment, that is the increments of the increments $\delta^2_\tau v_1(t) = \delta^1_\tau v_1(t+\tau) - \delta^1_\tau v_1(t)$, which is not only orthogonal to constants, but also to local linear trends, allowing in particular to estimate Hurst exponents greater than unity. We display in the inset of Fig. 2(a) the behavior of their second moment as a function of the scale τ. Once again, we observe a power-law behavior between the dissipative range, where $\langle(\delta^2_\tau v_1)^2\rangle \propto \tau^4$ and the large scales $\tau \gg T$ for which we get a saturation toward $6\langle v_1^2\rangle$. We fit the obtained exponents and reproduce our results in Fig. 2(c) (using □). In this case, we obtain a very convincing linear behavior, that falls in between H_{Eul} (dashed line) and $H_{\mathrm{Lag}} = H_{\mathrm{Eul}} + \frac{1}{6}$, that includes in particular the Kolmogorov's values $H_{\mathrm{Eul}} = 1/3$ and $H_{\mathrm{Lag}} = 1/2$ (represented by a solid black line). We performed the same analysis using the third-order increment, i.e., $\delta^3_\tau v_1(t) = \delta^2_\tau v_1(t+\tau) - \delta^2_\tau v_1(t)$, and obtain same results as with $\delta^2_\tau v_1$ (data not shown). We report in Figs. 2(b) and 2(d) a similar study, but with a frozen-in-time advection velocity field $\boldsymbol{u}(\boldsymbol{x}, 0)$, as it is illustrated in Figs. 1(b) and 1(d). The very same conclusions as in the time-evolving case can be drawn. In [29], we perform additional numerical simulations, using larger resolutions up to $N = 2^{16}$ collocation points of purely spatial advecting fields, that allow us to unambiguously eliminate the effects of regularization at small ϵ and large L scales, which confirm that $H_{\mathrm{Lag}} \approx H_{\mathrm{Eul}}$.

Let us finally quantify intermittent corrections on the trajectories (i.e., the dependence of H_{Lag} and γ_{Lag} on H_{Eul} and γ_{Eul}). To do so, we repeat former simulations for five values of the parameter γ_{Eul}. Recall that in a $3d$ turbulent field, $\gamma^2_{\mathrm{Eul}} \approx 0.025$ [14]. We start by performing a similar study as presented in Fig. 2, but with a varying γ_{Eul}, and found no differences with former conclusions: $H_{\mathrm{Lag}} \approx H_{\mathrm{Eul}}$, independently of γ_{Eul} (data not shown). This is a nontrivial property. Furthermore, trajectories extracted from a Gaussian field (i.e., $\gamma_{\mathrm{Eul}} = 0$) are intermittent. To see this, we display in Fig. 3(a) the probability density functions (PDFs) of Lagrangian velocity increments at various scales (using $H_{\mathrm{Eul}} = 1/3$ and $\gamma_{\mathrm{Eul}} = 0$). We indeed observe the continuous shape deformation of the PDFs, which is characteristic of the intermittency phenomenon [41]. Actually, these non-Gaussian behaviors were already seen on the typical time series of acceleration in Fig. 1(c). Note that at the smallest scale [top blue curve of Fig. 3(a)], PDFs of increments and acceleration coincide in this representation, and exhibit noticeable exponential tails, as they are obtained for pressure gradients in Gaussian ensembles [42]. At the same line, we represent in Fig. 3(b) the acceleration PDFs for varying γ_{Eul}, and for $H_{\mathrm{Eul}} = 1/3$. We see that as γ_{Eul} increases, the acceleration PDF develops larger and larger tails, which shows that γ_{Lag} increases in a monotonic way with γ_{Eul}. To quantify more precisely this dependence, we estimate the Lagrangian velocity flatness $\mathcal{F}^1(\tau) = \langle(\delta^1_\tau v_1)^4\rangle / \langle(\delta^1_\tau v_1)^2\rangle^2$ that is expected to behave,

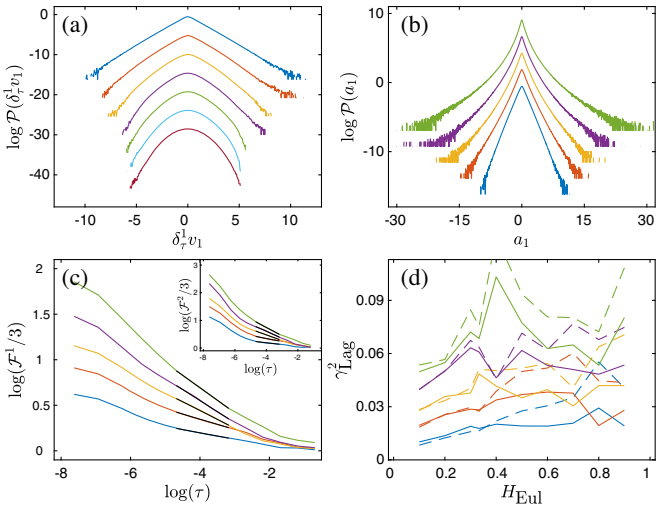

FIG. 3. (a) PDFs of the Lagrangian increments $\delta^1_\tau v_1$ from large (bottom) to small (top) scales in a Gaussian advecting field of parameters $H_{\mathrm{Eul}} = 1/3$ and $\gamma_{\mathrm{Eul}} = 0$. PDFs are all of unit variance, and arbitrarily shifted vertically for clarity. (b) PDFs of Lagrangian acceleration for $H_{\mathrm{Eul}} = 1/3$ and for $\gamma^2_{\mathrm{Eul}} = 0$, 0.01, 0.02, 0.03, and 0.04 (from bottom to top), of unit variance and arbitrarily shifted. (c) Logarithmic representation of the flatness of $\delta^1_\tau v_1$ (see text), with same parameters and colors as in (b). Inset: same as in (c), but for $\delta^2_\tau v_1$. Results of fitting are displayed with black lines. (d) Estimated values for γ_{Lag} [Eq. (6)] from the fitting procedure of the flatness curves of (c). Same colors as in (b) and (c), for $\delta^1_\tau v_1$ (solid lines) and $\delta^2_\tau v_1$ (dashed lines).

according to Eq. (6), as $\tau^{-4\gamma^2_{\mathrm{Lag}}}$ in the inertial range. We represent in Fig. 3(c) the behavior of the flatness for increasing values of γ_{Eul} and $H_{\mathrm{Eul}} = 1/3$. We see that flatness is close to three at large scales $\tau \sim T$, i.e., the value for a Gaussian process, and increases, all the more as γ_{Eul} gets bigger, as the scale decreases. The overall dependence of γ_{Lag} on both H_{Eul} and γ_{Eul} is illustrated in Fig. 3(d), where the estimation of γ_{Lag} is based on both the flatness of the first-order (solid lines) and second-order (dashed lines) increments. We can conclude to a complex dependence of γ_{Lag} on the parameters of the advecting Eulerian field. Interestingly, the Lagrangian intermittency coefficient in experimental and numerical $3d$ flows has been found compatible with $\gamma^2_{\mathrm{Lag}} \approx 0.085$ [7], a value which is of the order of what is found presently when we focus on the particular value $H_{\mathrm{Eul}} \approx 1/3$ and $\gamma^2_{\mathrm{Eul}} = 0.025$. We provide in [29] a similar study with a frozen-in-time advecting field that shows that obtained intermittent corrections on Lagrangian velocities are similar to those displayed in Fig. 3.

To summarize, we have built an incompressible statistically homogeneous, isotropic, and stationary spatio-temporal Eulerian advection field [Eq. (2)]. It is asymptotically rough and multifractal [Eq. (5)], governed at small scales by the parameters H_{Eul} and γ_{Eul}. We have then estimated, based on numerical simulations, the statistical properties of its Lagrangian trajectories. We find that

they are also asymptotically rough and multifractal [Eq. (6)], and relate their parameters H_{Lag} and γ_{Lag} to those of the advecting Eulerian field. In particular, we estimate with good accuracy, at second-order from a statistical point of view, that the regularity of the trajectories follows closely the one of the Eulerian field. Furthermore, we evidence unambiguous intermittent corrections, even when the advecting field is prescribed to be Gaussian. These are new and nontrivial results that are calling for new theoretical developments. In this regard, great progress has been made in the mathematical description of path lines of some rough advecting fields [43,44]. Also, the proposed velocity field could be used to investigate related important situations, such as the passive advection of scalars [22], and the relative dispersion of particle pairs [45,46]. Advecting fields of Ref. [20], some of which get rid of the sweeping by large scales, are explored in [29], and lead for some aspects to similar conclusions. Finally, including the intrinsically asymmetrical nature of the distributions of the advecting field (i.e., the skewness phenomenon), as it is proposed in Refs. [26,47], may allow to reproduce the observed values $H_{\mathrm{Eul}} = 1/3$ and $H_{\mathrm{Lag}} = 1/2$, possibly on the line $H_{\mathrm{Lag}} = H_{\mathrm{Eul}} + \frac{1}{6}$.

We warmly thank K. Gawedzki for many crucial discussions, M. Adda-Bedia and S. Ciliberto for a critical proofreading of the manuscript. L. C. is partially supported by the Simons Foundation Grant No. 651475.

*jason.reneuve@ens-lyon.fr

[1] P. K. Yeung and S. B. Pope, J. Fluid Mech. **207**, 531 (1989).
[2] G. A. Voth, K. Satyanarayan, and E. Bodenschatz, Phys. Fluids **10**, 2268 (1998).
[3] A. La Porta, G. A. Voth, A. M. Crawford, J. Alexander, and E. Bodenschatz, Nature (London) **409**, 1017 (2001).
[4] N. Mordant, P. Metz, O. Michel, and J.-F. Pinton, Phys. Rev. Lett. **87**, 214501 (2001).
[5] N. Mordant, J. Delour, E. Léveque, A. Arnéodo, and J.-F. Pinton, Phys. Rev. Lett. **89**, 254502 (2002).
[6] N. Mordant, J. Delour, E. Lévêque, O. Michel, A. Arneodo, and J.-F. Pinton, J. Stat. Phys. **113**, 701 (2003).
[7] L. Chevillard, S. G. Roux, E. Lévêque, N. Mordant, J.-F. Pinton, and A. Arneodo, Phys. Rev. Lett. **91**, 214502 (2003).
[8] R. Friedrich, Phys. Rev. Lett. **90**, 084501 (2003).
[9] L. Biferale, G. Boffetta, A. Celani, B. J. Devenish, A. Lanotte, and F. Toschi, Phys. Rev. Lett. **93**, 064502 (2004).
[10] J. Bec, L. Biferale, G. Boffetta, A. Celani, M. Cencini, A. Lanotte, S. Musacchio, and F. Toschi, J. Fluid Mech. **550**, 349 (2006).
[11] F. Toschi and E. Bodenschatz, Annu. Rev. Fluid Mech. **41**, 375 (2009).
[12] J.-F. Pinton and B. L. Sawford, in *Ten Chapters in Turbulence*, edited by P. A. Davidson, Y. Kaneda, and K. R. Sreenivasan (Cambridge University Press, Cambridge, 2012), pp. 132–175.
[13] L. Bentkamp, C. Lalescu, and M. Wilczek, Nat. Commun. **10**, 3550 (2019).
[14] U. Frisch, *Turbulence, The Legacy of A. N. Kolmogorov* (Cambridge University Press, Cambridge, England, 1995).
[15] H. Tennekes and J. L. Lumley, *A First Course in Turbulence* (MIT Press, Cambridge, 1972).
[16] A. N. Kolmogorov, Dokl. Akad. Nauk SSSR **30**, 301 (1941).
[17] T. Komorowski and G. Papanicolaou, Ann. Appl. Probab. **7**, 229 (1997).
[18] J. C. H. Fung and J. C. Vassilicos, Phys. Rev. E **57**, 1677 (1998).
[19] A. Fannjiang and T. Komorowski, Ann. Appl. Probab. **10**, 1100 (2000).
[20] M. Chaves, K. Gawedzki, P. Horvai, A. Kupiainen, and M. Vergassola, J. Stat. Phys. **113**, 643 (2003).
[21] M. Khan and J. Vassilicos, Phys. Fluids **16**, 216 (2004).
[22] G. Falkovich, K. Gawedzki, and M. Vergassola, Rev. Mod. Phys. **73**, 913 (2001).
[23] R. Robert and V. Vargas, Commun. Math. Phys. **284**, 649 (2008).
[24] L. Chevillard, R. Robert, and V. Vargas, Europhys. Lett. **89**, 54002 (2010).
[25] R. M. Pereira, C. Garban, and L. Chevillard, J. Fluid Mech. **794**, 369 (2016).
[26] L. Chevillard, C. Garban, R. Rhodes, and V. Vargas, Ann. Henri Poincaré **20**, 3693 (2019).
[27] J. Reneuve, Modeling of the fine structure of quantum and classical turbulence, Ph.D. thesis, Université de Lyon, 2019.
[28] A. Majda and A. Bertozzi, *Vorticity and Incompressible Flow* (Cambridge University Press, Cambridge, England, 2002).
[29] See Supplemental Material at http://link.aps.org/supplemental/10.1103/PhysRevLett.125.014502 for technical details, alternative propositions, and additional numerical simulations, which includes Refs. [30,31].
[30] B. B. Mandelbrot and J. W. Van Ness, SIAM Rev. **10**, 422 (1968).
[31] A. Arneodo *et al.*, Phys. Rev. Lett. **100**, 254504 (2008).
[32] C. Meneveau and K. R. Sreenivasan, Phys. Rev. Lett. **59**, 1424 (1987).
[33] R. Benzi, L. Biferale, A. Crisanti, G. Paladin, M. Vergassola, and A. Vulpiani, Physica (Amsterdam) **65D**, 352 (1993).
[34] A. Arneodo, E. Bacry, and J.-F. Muzy, J. Math. Phys. (N.Y.) **39**, 4142 (1998).
[35] R. Rhodes and V. Vargas, Probab. Surv. **11**, 315 (2014).
[36] J. Barral and B. B. Mandelbrot, Probab. Theory Relat. Fields **124**, 409 (2002).
[37] F. Schmitt and D. Marsan, Eur. Phys. J. B **20**, 3 (2001).
[38] E. Bacry and J.-F. Muzy, Commun. Math. Phys. **236**, 449 (2003).
[39] H. Yu, K. Kanov, E. Perlman, J. Graham, E. Frederix, R. Burns, A. Szalay, G. Eyink, and C. Meneveau, J. Turbul. **13**, 1 (2012).
[40] L. Chevillard, S. G. Roux, E. Lévêque, N. Mordant, J.-F. Pinton, and A. Arnéodo, Phys. Rev. Lett. **95**, 064501 (2005).
[41] B. Castaing, Y. Gagne, and E. Hopfinger, Physica (Amsterdam) **46D**, 177 (1990).

[42] M. Holzer and E. Siggia, Phys. Fluids A **5**, 2525 (1993).
[43] J. Dubédat, J. Am. Math. Soc. **22**, 995 (2009).
[44] J. Miller and S. Sheffield, Probab. Theory Relat. Fields **164**, 553 (2016).
[45] M. Bourgoin, N. T. Ouellette, H. Xu, J. Berg, and E. Bodenschatz, Science **311**, 835 (2006).
[46] R. Bitane, H. Homann, and J. Bec, Phys. Rev. E **86**, 045302(R) (2012).
[47] J.-F. Muzy, Phys. Rev. E **99**, 042113 (2019).